JOURNAL OF PROPULSION AND POWER
Vol. 10, No. 3, May–June 1994

Low-Noise, High-Strength, Spiral-Bevel Gears for Helicopter Transmissions

David G. Lewicki* and Robert F. Handschuh*
NASA Lewis Research Center, Cleveland, Ohio 44135
Zachary S. Henry†
Bell Helicopter Textron, Inc., Fort Worth, Texas 76101
and
Faydor L. Litvin‡
University of Illinois at Chicago, Chicago, Illinois 60680

Advanced-design spiral-bevel gears were tested in an OH-58D helicopter transmission using the NASA 500-hp Helicopter Transmission Test Stand. Three different gear designs tested included 1) the current design of the OH-58D transmission; 2) a higher-strength design the same as the current but with a full fillet radius to reduce gear tooth bending stress (and thus, weight); and 3) a lower-noise design the same as the high-strength but with modified tooth geometry to reduce transmission error and noise. Noise, vibration, and tooth strain tests were performed and significant gear stress and noise reductions were achieved.

Introduction

SPIRAL-BEVEL gears are used extensively in rotorcraft applications to transfer power and motion through nonparallel shafts. In helicopter applications, spiral-bevel gears are used in main-rotor and tail-rotor gearboxes to drive the rotors. In tilt-rotor applications, they are used in interconnecting drive systems to provide mechanical connection between two prop-rotors in case one engine becomes inoperable. Even though spiral-bevel gears have had considerable success in these applications, they are a main source of vibration in gearboxes, and therefore, a main source of noise in cabin interiors.[1,2] In addition, higher strength and lower weight are required to meet the needs of future aircraft.[3] An effort to improve the technology of components such as spiral-bevel gears has been the Advanced Rotorcraft Transmission (ART) program.

The intent of the ART program was to develop and demonstrate lightweight, quiet, durable drive systems for next generation rotorcraft.[4] The success of the ART design configurations in meeting the program goals of reduced weight and noise and increased life depended on the successful incorporation of certain critical, advanced technologies into the preliminary designs. A joint project to improve spiral-bevel gears was initiated. The project goals were to reduce bevel gear noise and increase strength through changes in gear tooth surface geometry, and tooth fillet and root designs.[5,6]

Various investigators have studied spiral-bevel gears and their influence on vibration and noise.[7–9] Most agree that transmission error, defined as the difference in relative motion of an output gear with respect to the input pinion, is the major contributor to undesirable vibration and noise. A common practice is to modify spiral-bevel gear surface topology to permit operation in a misaligned mode. Overcompensation for this type of operation, however, leads to large transmission error and higher noise and vibration levels. Gears with tooth surfaces designed for reduced transmission errors using methods of Litvin and Zhang[7] were manufactured and tested. The teeth were designed to exhibit a parabolic function of transmission error at a controlled low level (8–10 arcsec). The low level of transmission error reduces the vibration and noise caused by the mesh. The new tooth geometries for this design were achieved through slight modification of the machine tool settings used in the manufacturing process. The design analyses addressed tooth generation, tooth contact analysis, transmission error prediction, and effects of misalignment.[7,10,11]

In addition, gears with tooth fillet and root modifications to increase strength were manufactured and tested. By increasing these radii, reduced stresses were achieved, and thus, increased strength. Tooth fillet radii larger than those on current gears were made possible by recent advances in spiral-bevel gear grinding technology.[12] Advanced gear grinding was achieved through the redesigning of a current gear grinder and the addition of computer numerical control.

The objective of this article is to describe the results of the experiments to evaluate advanced spiral-bevel gear designs. Experimental tests were performed on the OH-58D helicopter main-rotor transmission in the NASA 500-hp Helicopter Transmission Test Stand. The baseline OH-58D spiral-bevel gear design, a low-noise design, and a high-strength design were tested. Results of noise, vibration, and tooth strain tests are presented.

Apparatus

OH-58D Main-Rotor Transmission

The OH-58 Kiowa is an Army single-engine, light, observation helicopter. The OH-58D is an advanced version developed under the Army Helicopter Improvement Program (AHIP). The OH-58D main-rotor transmission is shown in Fig. 1. It is currently rated at maximum continuous power of 346 kW (464 hp) at 6016 rpm input speed, with the capability of 10-s torque transients to 485 kW (650 hp), occurring once per hour, maximum. The main-rotor transmission is a two-stage reduction gearbox with an overall reduction ratio of 15.23:1. The first stage is a spiral-bevel gear set with a 19-tooth pinion that meshes with a 62-tooth gear. Triplex ball bearings and one roller bearing support the bevel-pinion shaft. Duplex ball bearings and one roller bearing support the bevel-gear shaft. Both pinion and gear are straddle mounted.

Received April 15, 1993; presented as Paper 93-2149 at the AIAA/SAE/ASME/ASEE 29th Joint Propulsion Conference, Monterey, CA, June 28, 1993; revision received Oct. 29, 1993; accepted for publication Nov. 19, 1993.

*Aerospace Engineer, U.S. Army Research Laboratory, Vehicle Propulsion Directorate.
†Engineering Specialist, Drive System Design Group.
‡Professor, Department of Mechanical Engineering.

Table 1 Baseline spiral-bevel gear design parameters of the OH-58D main-rotor transmission

Number of teeth	
Pinion	19
Gear	62
Diametral pitch	6.092
Pressure angle, deg	20
Mean spiral angle, deg	35
Shaft angle, deg	95
Face width, mm (in.)	36.83 (1.450)
Fillet radius, mm (in.)	
Pinion	0.51 (0.020)
Gear	1.65 (0.065)

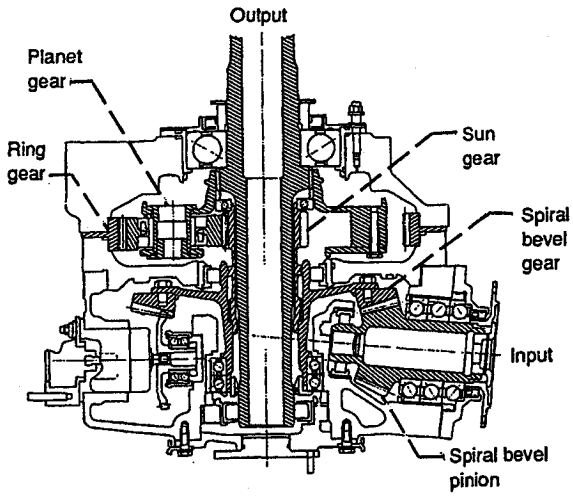

Fig. 1 OH-58D helicopter main-rotor transmission.

A planetary mesh provides the second reduction stage. The bevel-gear shaft is splined to a sun gear shaft. The 27-tooth sun gear meshes with four 35-tooth planet gears, each supported with cylindrical roller bearings. The planet gears mesh with a 99-tooth fixed ring gear splined to the transmission housing. Power is taken out through the planet carrier splined to the output mast shaft. The output shaft is supported on top by a split-inner-race ball bearing, and on bottom by a roller bearing. The 62-tooth bevel gear also drives a 27-tooth accessory gear. The accessory gear runs an oil pump, which supplies lubrication through jets and passageways located in the transmission housing.

The OH-58D transmission was tested in the NASA Lewis 500-hp Helicopter Transmission Test Stand[1] which operates on the closed-loop or torque-regenerative principle.

Spiral-Bevel Test Gears

Three different spiral-bevel gear designs were tested. The first was the baseline OH-58D design. Table 1 lists a variety of parameters for this baseline set. The reduction ratio of the bevel set is 3.26:1. The gears were made using standard aerospace practices where the surfaces were carburized and ground. The material used for all test gears was X-53 (AMS 6308) rather than the conventional AISI 9310 (AMS 6265).

The second spiral-bevel design tested was an increased strength design. The configuration was identical to the baseline except that the tooth fillet radius of the pinion was increased from 0.51 to 1.02 mm (0.020 to 0.040 in.), and the gear was made full fillet (Fig. 2). The high-strength design was made possible by recent advances in gear grinding technology.[12]

The third spiral-bevel design tested was a low-noise design. The low-noise design was identical to the increased-strength

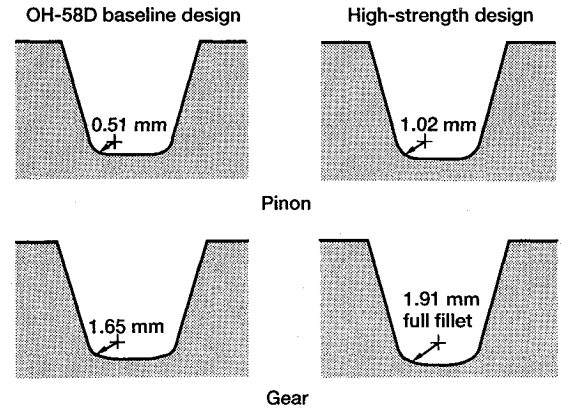

Fig. 2 Comparison of OH-58D and high-strength spiral-bevel gear designs.

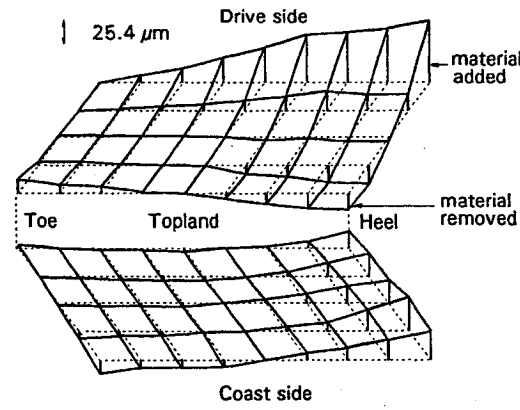

Fig. 3 Topological comparison of OH-58D and low-noise spiral-bevel pinion. ----- OH-58D baseline design, —— low-noise design.

design except the pinion was slightly altered to reduce transmission error. The gear member was unchanged. The low-noise design was based on the idea of local synthesis that provided at the mean contact point the following conditions of meshing and contact[7]: 1) the required gear ratio and its derivative, 2) the desired direction of the tangent to the contact path, and 3) the desired major axis of the instantaneous contact ellipse. The local synthesis was complemented with a tooth contact analysis. Using this approach, the machine tool settings for reduced noise were determined. As with the high-strength design, precise control of the manufactured tooth surfaces were made possible by advances in the final grinding operation machine tool.[12] Figure 3 gives a topological comparison between a low-noise and baseline spiral-bevel pinion tooth. The dotted lines are the baseline tooth datum, and the solid lines are the measured difference in topology of a low-noise gear compared to the baseline. Solid lines above the dotted plain indicate an addition of material, and lines below the plain indicate a removal. The effect of the topological change in the low-noise design was a reduction in overall crowning of the tooth, leading to an increase in contact ratio and reduced transmission error.

Test Procedure

Two sets of the baseline design, two sets of the high-strength design, and one set of the low-noise design were manufactured and tested. Noise and vibration tests were performed on all sets of each design. One set of the baseline design and one set of the high-strength design was instrumented with strain gauges and strain tests were performed on these gears. A description of the instrumentation, test procedure, and data reduction procedure is as follows.

Noise Tests

Acoustic intensity measurements were performed using the two-microphone technique. The microphones used had a flat

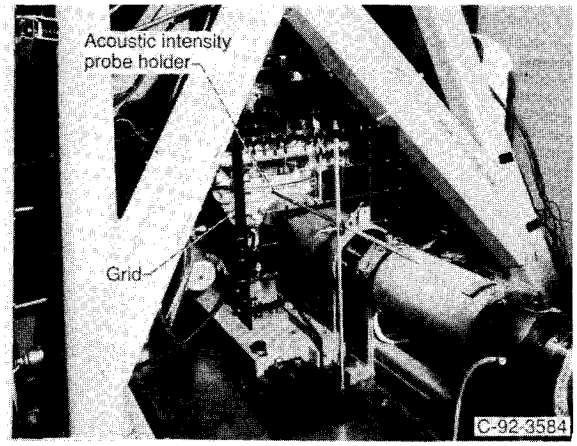

Fig. 4 Grid for sound intensity measurements.

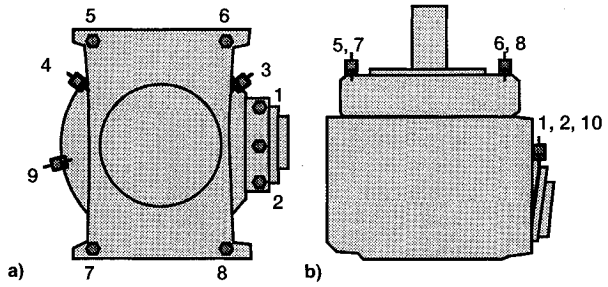

Fig. 5 Accelerometer locations on OH-58D transmission: a) top view and b) side view.

response (±2 dB) up to 5000 Hz and a nominal sensitivity of 50 mV/Pa. The microphones were connected to a spectrum analyzer which computed the acoustic intensity from the imaginary part of the cross-power spectrum. Near the input region of the OH-58D transmission, a grid was installed which divided the region into 16 areas (Fig. 4). For each test, the acoustic intensity was measured at the center of each of the 16 areas. Only positive acoustic intensities (noise flowing out of the areas) were considered. The acoustic intensities were then added together and multiplied by the total area of the grids to obtain sound power of the transmission input region.

At the start of each test, the test transmission oil was heated using an external heater and pumping system. For all the tests, the oil used conformed to a DOD-L-85734 specification. Once the oil was heated, the transmission input speed was increased to 3000 rpm, a nominal amount of torque was applied, and mast lift load was applied to align the input shaft (18,310 N, 4120 lb). The transmission input speed and torque were then increased to the desired conditions. The tests were performed at 100% transmission input speed (6016 rpm) and torques of 50, 75, 100, and 125% of maximum design. The transmission oil inlet temperature was set at 99°C (210°F). After the transmission oil outlet stabilized (which usually required about 20 min), the acoustic intensity measurements were taken. The time to obtain the acoustic intensity measurements of the 16 grid points was about 30 min. For each acoustic intensity spectrum at a grid point, 100 frequency-domain averages were taken. This data was collected by a computer. The computer also computed the sound power spectrum of the grids after all the measurements were taken.

Vibration Tests

Ten piezoelectric accelerometers were mounted at various locations on the OH-58D transmission housing (Fig. 5). The accelerometers were located near the input spiral-bevel area (accelerometers 1, 2, and 10, measuring radially to the input shaft), the ring gear area (3, 4, and 9, measuring radially to the planetary), and on the top cover (5 to 8, measuring vertically). Accelerometers 1–8 had a 1–25,000-Hz (±3-dB) response, 4-mV/g sensitivity, and integral electronics. Accelerometers 9 and 10 had a 2–6000-Hz (±5%) response and required charge amplifiers.

The vibration tests were performed in conjunction with the noise tests. After collecting the acoustic intensity data for a given test, the vibration data were recorded on tape and processed off-line. The vibration data were later analyzed using time averaging. Here, the vibration data recorded on tape were input to a signal analyzer along with a tach pulse from the transmission input shaft. The signal analyzer was triggered from the tach pulse to read the vibration data when the transmission input shaft was at the same position. The vibration signal was then averaged in the time domain using 100 averages. This technique removed all the vibration which was not synchronous to the input shaft. Before averaging, the major tones in the vibration spectrum of the OH-58D baseline design were the spiral-bevel and planetary gear fundamental frequencies and harmonics. Time averaging removed the planetary contribution, leaving the spiral-bevel contribution for comparing the different design configurations.

Strain Tests

Twenty strain gauges were mounted on the spiral-bevel pinions, and 26 gauges were mounted on the spiral-bevel gears of one set each of the baseline and high-strength designs (Figs. 6 and 7). Gauges were positioned evenly across the tooth face widths with some in the fillet area and some in the root area of the teeth. The fillet gauges were placed on the drive side of the teeth. The fillet gauges were also positioned at a point on the tooth cross section where a line at a 45-deg angle with respect to the tooth centerline intersects the tooth profile (Fig. 6b). The fillet gauges were placed there to measure maximum tooth bending stress. Previous studies on spur gears showed that the maximum stresses were at a line 30 deg to the tooth

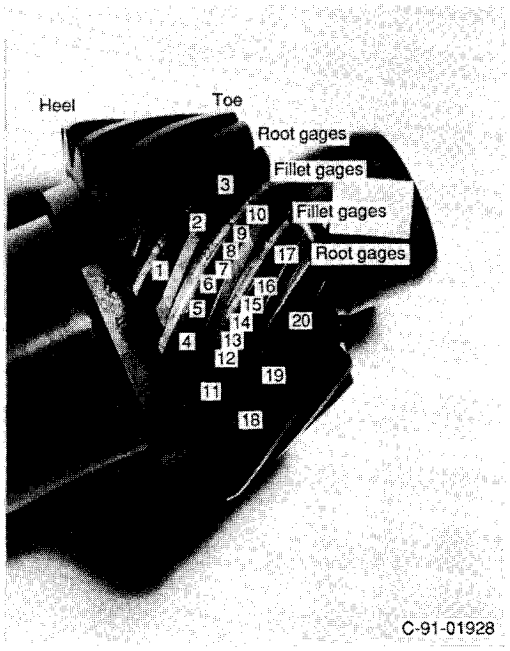

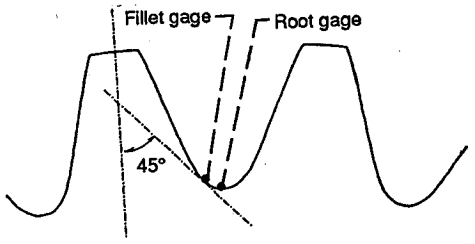

Fig. 6 Strain gauge locations on spiral-bevel pinion: a) gauge numbering and b) cross-sectional view.

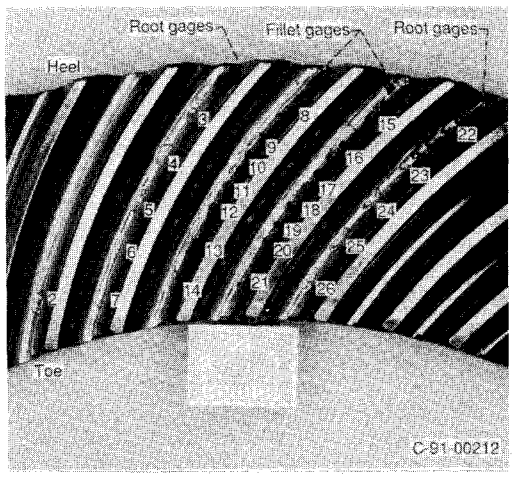

Fig. 7 Strain gauge locations on spiral-bevel gear.

centerline.[13] 45-Deg was chosen for the current tests to minimize the possibility of the gauges being destroyed due to tooth contact. In addition to maximum tensile stresses, root stresses can become significant in lightweight, thin-rimmed aerospace gear applications.[14] Thus, root gauges were centered between teeth in the root to measure gear rim stress. Tooth fillet and root gauges were placed on successive teeth to determine loading consistency. The grid length of the gauges was 0.381 mm (0.015 in.), and the nominal resistance was 120 Ω. The gauges were connected to conditioners using a Wheatstone bridge circuitry and using a quarter-bridge arrangement.

Static strain tests were performed on both the spiral-bevel pinions and gears. A crank was installed on the transmission input shaft to manually rotate the shaft to the desired position. A sensor was installed on the transmission output shaft to measure shaft position. At the start of a test, the transmission was completely unloaded and the strain gauge conditioners were zeroed. Conditioner spans were then determined using shunt calibrations. The transmission was loaded (using the facility closed-loop system) to the desired torque, the shaft was positioned, and the strain readings were obtained using a computer. This was done for a variety of positions to get strain as a function of shaft position for the different gauges. At the end of a test, the transmission was again completely unloaded and the conditioner zeroes were checked for drift. All static tests were performed at room temperature.

Dynamic strain tests were performed only on the spiral-bevel pinions. The pinion gauges were connected to slip rings mounted on the input shaft. A slip ring assembly for the spiral-bevel gear was unavailable, and thus, dynamic strain tests of the gear were not performed. The test procedure was basically the same as the noise and vibration tests, except that the transmission was not run as long in order to maximize strain gauge life.

Results and Discussion

Noise Tests

The noise spectrum (sound power vs frequency) at 100% torque is given in Fig. 8. The results shown are for set 1 of the baseline configuration and set 1 of the low-noise configuration. Among the dominant spikes in the spectrum for the baseline design are the spiral-bevel meshing frequency (1905 Hz) and second harmonic (3810 Hz). Note that these tones are significantly reduced for the low-noise design. Other dominant tones in the spectrum are at the planetary meshing frequencies (fundamental at 652 Hz). The planetary tones were not affected by the low-noise design. Tones from the facility closing-end gearbox were also dominant in the spectrum (fundamental at 790 Hz), and as expected were not affected by the low-noise design.

The effect of torque on sound power at the spiral-bevel frequencies is given in Fig. 9. Both sets of the baseline and high-strength designs and one set of the low-noise design are included. The sound power is the cumulation of the spiral-bevel meshing frequency (1905 Hz) and second harmonic (3810 Hz). The baseline and high-strength designs produced basically the same noise since the difference between them was in the tooth fillet geometry. There was some scatter in the baseline and high-strength results due to manufacturing tolerances of the different sets and assembly tolerances. To check assembly tolerances, the low-noise tests were repeated two times. Here, the gears were completed disassembled and reassembled in the transmission, and the tests were repeated. The results showed the same trend and were repeatable to within about 2 dB. The general trend was a significant decrease in spiral-bevel gear noise for the low-noise design compared to the baseline and high-strength design. At 100% torque, the noise due to the spiral-bevel mesh was 12–19 dB lower than that of the baseline and high-strength designs. Also, a decrease in noise was most prevalent at 100 and 125% torque, and less prevalent at 50 and 75% torque.

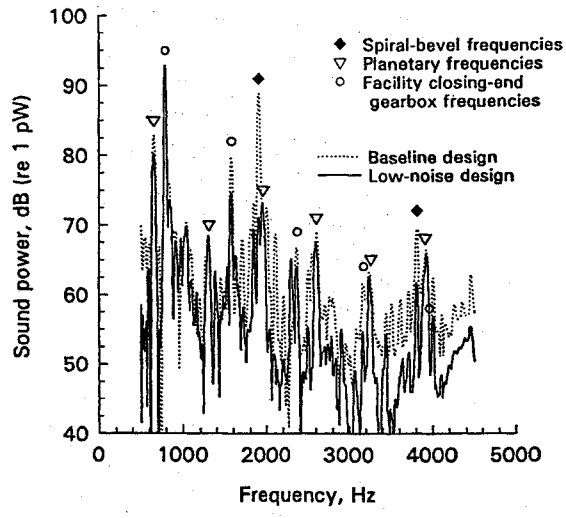

Fig. 8 Noise spectrum; test at 100% torque.

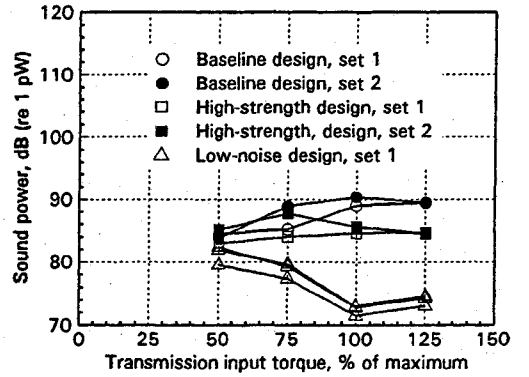

Fig. 9 Noise test results; sound power at spiral-bevel mesh frequencies (first two harmonics) vs transmission input torque.

Vibration Results

The vibration spectrum (time-averaged acceleration vs frequency) for accelerometer 1 (input spiral-bevel housing) at 100% torque is given in Fig. 10. As with Fig. 8, the results compare set 1 of the baseline to set 1 of the low-noise configuration. The figure clearly shows the dominant spikes for the baseline design at the spiral-bevel meshing frequencies, and the significant reduction in spiral-bevel gear vibration for the low-noise design. The results of the other nine accelerometers were similar.

The effect of torque on vibration for accelerometer 1 is given in Fig. 11. Shown in the figure is time-averaged acceleration processed up to 10,000 Hz. The results are root-mean-

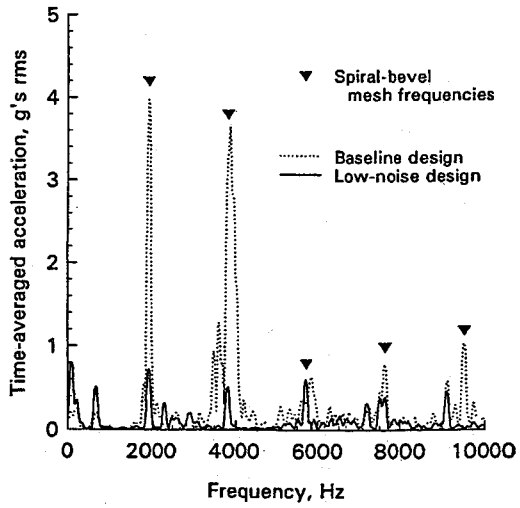

Fig. 10 Vibration spectrum; accelerometer 1, test at 100% torque.

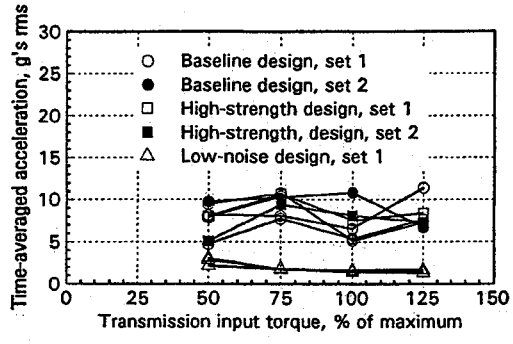

Fig. 11 Typical vibration test results, accelerometer 1, input spiral-bevel housing.

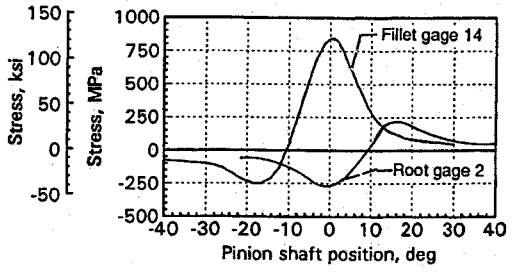

Fig. 12 Typical strain test results; spiral-bevel pinion, 100% torque.

square (rms) calculations of the time-domain signals. Since the time-averaging removed vibration nonsynchronous to the input shaft, the results in Fig. 11 were basically the cumulation of the spiral-bevel meshing frequency (1905 Hz) and second through fifth harmonics.

As with the noise measurements, the vibration for the baseline and high-strength designs were similar, but with scatter. Again, the figure clearly shows a significant reduction in spiral-bevel gear vibration for the low-noise design compared to the baseline and high-strength designs. Like the noise results, the reduction in vibration for the low-noise design was greater at the higher torques (100 and 125%). The results of the other nine accelerometers were similar. From the results of all 10 accelerometers and at 100% torque, the vibration for the low-noise design due to the spiral-bevel mesh was on the average 5–10g lower than that of the baseline and high-strength designs.

Strain Tests

Figure 12 shows the results of a typical static strain test of the spiral-bevel pinion. A uniaxial stress field was assumed to exist at the strain gauge and the stress was determined by multiplying the measured strain by Young's modulus for steel. For a pinion fillet gauge, the stress was first compressive, then tensile. Since the pinion drove the gear, the compression occurred when the tooth in mesh prior to the strain-gauged tooth was loaded, causing compression in the gauge. As the pinion rotated, the strain-gauged tooth was loaded in single-tooth contact and the gauge measured the maximum tensile stress. Similar conditions existed for the pinion root gauge, except the gauge measured the stress of the pinion rim rather than tooth bending. The results for the spiral-bevel gear were similar to the pinion, except the tensile stress occurred before the compression since the pinion drove the gear.

Figure 13 shows the distribution of maximum tensile and compressive stress during contact along the tooth face width for the baseline and high-strength designs. The most important item to note is the reduction in maximum tensile bending stress of the high-strength design compared to the baseline design. The maximum tensile stress of the high-strength design was reduced on the average 27% compared to the baseline for the spiral-bevel pinion (Fig. 13a). There was, however, an increase in the maximum compressive fillet stress for the spiral-bevel pinion. Thus, the alternating stress of the high-strength design was reduced on the average 14% compared to the baseline (the alternating stress is defined as the maximum tensile stress plus the absolute value of the maxi-

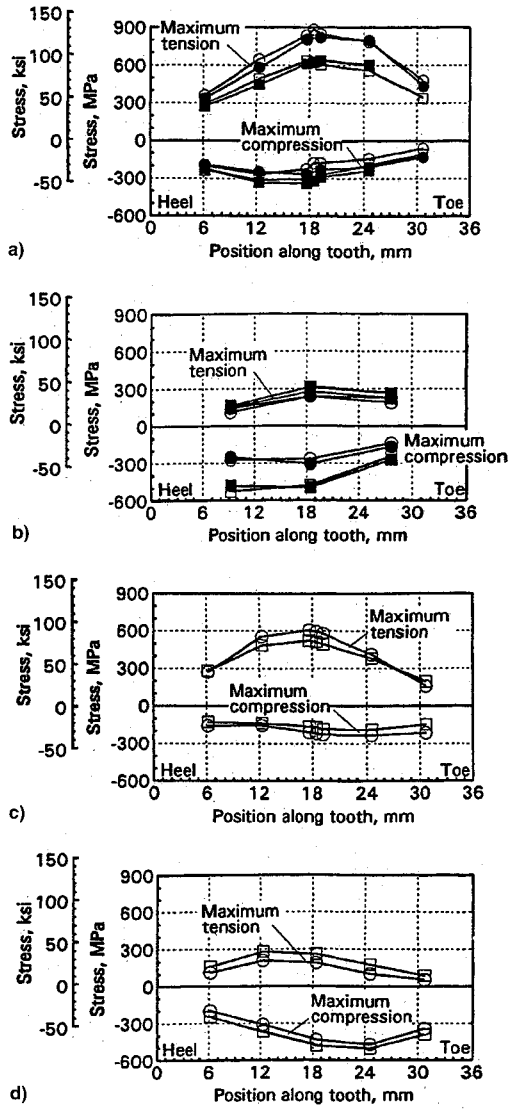

Fig. 13 Strain test results; 100% torque: a) spiral-bevel pinion fillet gauges, b) spiral-bevel pinion root gauges, c) spiral-bevel gear fillet gauges, and d) spiral-bevel gear root gauges. ○, Baseline design, static tests; ● baseline design, dynamic tests; □, high-strength design, static tests; and ■, high-strength design, dynamic tests.

mum compressive stress). For the spiral-bevel gear, the maximum tensile stress of the high-strength design was reduced on the average 10% compared to the baseline, and the alternate was reduced on the average 12% (Fig. 13c). Thus, the increase in fillet radii of the high-strength design has a significant benefit in increasing the tooth bending capacity of the gear tooth.

There was a significant increase in the maximum compressive root stress of the high-strength design compared to the baseline spiral-bevel pinion (Fig. 13b), and a slight increase for the gear (Fig. 13d). This was probably due to the removal of material for the increased fillet, thus lowering the rim thickness. For the OH-58D design, this increase in stress is acceptable, but in general, these effects need to be considered in a design.

Figure 13 also shows the results of the dynamic strain tests for the spiral-bevel pinion. The results of the dynamic strain tests matched closely to those of the static. The stress-position plots were similar as well as the maximum and minimum stresses, indicating no detrimental dynamic effects.

Summary of Results

Advanced-design spiral-bevel gears were tested in an OH-58D helicopter transmission using the NASA 500-hp Helicopter Transmission Test Stand. Three different gear designs were tested. The baseline design was the current design of the OH-58D transmission. The second design was a higher-strength design which was the same as the baseline, but incorporated a full fillet radius to reduce gear tooth bending stress. The third design was a lower-noise design which was the same as the high-strength design, except the tooth geometry was modified to reduce transmission error and noise. Noise, vibration, and tooth strain tests were performed. The following results were obtained:

1) For the baseline spiral-bevel gear design, dominant tones in the noise and vibration spectra occurred at the spiral-bevel meshing frequencies and harmonics. A significant decrease in the spiral-bevel tones resulted from the low-noise design. At 100% torque, the noise (sound power) due to the spiral-bevel meshing frequencies of the low-noise design was 12–19 dB lower than that of the baseline and high-strength designs. Using a time-average processing scheme, the spiral-bevel gear vibration of the low-noise design was 5–10g lower than that of the baseline and high-strength designs.

2) The increased fillet radius of the high-strength design had a significant benefit in decreasing tooth bending stress. For tests at 100% torque, the spiral-bevel pinion maximum tooth bending stress of the high-strength design was on the average 27% lower than that of the baseline design. There was, however, an increase in the maximum compressive stress at the center of the tooth root.

References

[1]Lewicki, D. G., and Coy, J. J., "Vibration Characteristics of OH-58A Helicopter Main Rotor Transmission," NASA TP-2705, April 1987.

[2]Mitchell, A. M., Oswald, F. B., and Coe, H. H., "Testing of UH-60A Helicopter Transmission in NASA-Lewis 2240-kW (3000-hp) Facility," NASA TP-2626, Aug. 1986.

[3]Vialle, M., "Tiger MGB-, High Reliability-, Low Weight," *Proceedings of the 47th American Helicopter Society Annual Forum Proceedings*, Vol. 2, AHS, Alexandria, VA, 1991, pp. 1249–1258.

[4]Bill, R. C., "Advanced Rotorcraft Transmission Program," NASA TM-103276, May 1990.

[5]Henry, Z. S., "Preliminary Design and Analysis of an Advanced Rotorcraft Transmission," *Proceedings of the AIAA/ASME/SAE/ASEE 27th Joint Propulsion Conference*, AIAA, Washington, DC, 1991, pp. 1–14.

[6]Henry, Z. S., "Advanced Rotorcraft Transmission (ART)—Component Test Results," AIAA/ASME/SAE 28th Joint Propulsion Conf., Nashville, TN, July 1992.

[7]Litvin, F. L., and Zhang, Y., "Local Synthesis and Tooth Contact Analysis of Face-Milled Spiral Bevel Gears," NASA CR-4342, Jan. 1991.

[8]Gosselin, C., Cloutier, L., and Brousseau, J., "Tooth Contact Analysis of High Conformity Spiral Bevel Gears," *Proceedings of the International Conference on Motion and Power Transmissions* (Hiroshima, Japan), Japan Society of Mechanical Engineers, Tokyo, Japan, Nov. 1991, pp. 725–730.

[9]Fong, Z. H., and Tsay, C. B., "Kinematic Optimization of Spiral Bevel Gears," *Journal of Mechanical Design*, Vol. 114, No. 3, 1992, pp. 498–506.

[10]Litvin, F. L., Zhang, Y., and Chen, J., "User's Manual for Tooth Contact Analysis of Face-Milled Spiral Bevel Gears with Given Machine-Tool Settings," NASA CR-189093, Dec. 1991.

[11]Litvin, F. L., Kuan, C., and Zhang, Y., "Determination of Real Machine-Tool Settings and Minimization of Real Surface Deviation by Computer Inspection," NASA CR-4383, July 1991.

[12]Scott, H. W., "Computer Numerical Control Grinding of Spiral Bevel Gears," NASA CR-187175, Aug. 1991.

[13]Hirt, M. C. O., "Stress in Spur Gear Teeth and Their Strength as Influenced by Fillet Radius," Ph.D. Dissertation, Technische Univ. München, Munich, Germany (translated by the American Gear Manufacturers Association), 1976.

[14]Drago, R. J., "Design Guidelines for High-Capacity Bevel Gear Systems," AE-15 Gear Design, Manufacturing and Inspection Manual, Society of Automotive Engineers, Warrendale, PA, 1990, pp. 105–121.